Journal of Basic Microbiology
Environment · Health · Techniques

Research Paper

Acute dextran sulfate sodium (DSS)-induced colitis promotes gut microbial dysbiosis in mice

Peris Mumbi Munyaka[1,2], Mohammad Fazle Rabbi[1], Ehsan Khafipour[2,3] and Jean-Eric Ghia[1,4,5]

[1] Department of Immunology, University of Manitoba, Winnipeg, Manitoba, Canada
[2] Department of Animal Science, University of Manitoba, Winnipeg, Manitoba, Canada
[3] Department of Medical Microbiology, University of Manitoba, Winnipeg, Manitoba, Canada
[4] Department of Internal Medicine, Section of Gastroenterology, University of Manitoba, Winnipeg, Manitoba, Canada
[5] Inflammatory Bowel Disease Clinical & Research Centre, University of Manitoba, Winnipeg, Manitoba, Canada

The most widely used and characterized experimental model of ulcerative colitis (UC) is the epithelial erosion, dextran sulfate sodium (DSS)-induced colitis, which is developed by administration of DSS in drinking water. We investigated fecal and colonic mucosa microbial composition and functional changes in mice treated with DSS. C57Bl/6 mice received 5% DSS in drinking water for 5 days. Inflammation was evaluated clinically and by analysis of colonic tissue cytokine levels and C-reactive protein (CRP) in the serum. Colonic mucosa and fecal samples were used for DNA extraction and the V4 region of bacterial 16S rRNA gene was subjected to MiSeq Illumina sequencing. Alpha- and beta-diversities, and compositional differences at phylum and genus levels were determined, and bacterial functional pathways were predicted. DSS increased disease severity, serum CRP and cytokines IL-1β and IL-6, but decreased bacterial species richness, and shifted bacterial community composition. *Bacteroides*, *Turicibacter*, *Escherichia*, *Clostridium*, Enterobacteriaceae, Clostridiaceae, Bacteroidaceae, Bacteroidales, among other taxa were associated with DSS treatment in fecal and colonic samples. Also, DSS altered microbial functional pathways in both colonic mucosa and fecal samples. Conclusions: The development of colitis in DSS model was accompanied with reduced microbial diversity and dysbiosis of gut microbiota at lower taxonomical levels.

Abbreviations: CD – Crohn's disease; CRP – C-reactive protein; DAI – disease activity index; DSS – dextran sodium sulfate; IBD – inflammatory bowel diseases; IL – interleukin; OTU – operational taxonomic unit; PLS-DA – partial least square discriminant analysis; UC – ulcerative colitis

Keywords: Colitis / Dextran sulfate sodium / Dysbiosis / Mice / Microbiota

Received: December 3, 2015; accepted: March 18, 2016

DOI 10.1002/jobm.201500726

Introduction

Ulcerative colitis (UC) and Crohn's disease (CD) represent the two major forms of inflammatory bowel disease (IBD) that are characterized by alternating phases of clinical relapse and remission [1–3]. The etiology of both CD and UC is unclear; however, accumulating data suggest that a genetic predisposition or a combination of genetic susceptibility factors (e.g., CARD15/NOD2, JAK-2/STAT3) [4], defective mucosal barrier [5, 6], altered innate and adaptive immune responses and their interactions with commensal gut microbiota in the enteric environment [4, 7, 8], and different environmental factors contributes to the initiation and the recurrence of these diseases.

Much of the recent progress in the understanding of immunity has been achieved using experimental animal models of intestinal inflammation [9–11]. Although these models do not represent the complexity of human

Peris Mumbi Munyaka and Mohammad Fazle Rabbi contributed equally to this work.

Correspondence: Dr. Jean-Eric Ghia, Departments of Immunology and Internal Medicine, Section of Gastroenterology, College of Medicine, University of Manitoba, 750 McDermot Avenue, Winnipeg, Manitoba R3E 0T5, Canada
E-mail: jean-eric.ghia@umanitoba.ca
Correspondence: Dr. Ehsan Khafipour, Department of Animal Science, University of Manitoba, 12 Dafoe Road, Winnipeg, Manitoba R3T 2N2, Canada
E-mail: ehsan.Khafipour@umanitoba.ca

disease and do not replace studies with patient samples, they are valuable tools for studying many important disease aspects that are difficult to address in humans and they, therefore, provide a platform through which some of the complex mechanisms can be systematically investigated [12]. Most of these models require exogenous manipulation based either on chemical induction, immune cell transfer or gene targeting [9–11, 13], and only a few models occur spontaneously without any exogenous manipulation [13–15]. Chemically induced models of intestinal inflammation are among the most commonly used animal models of IBD as the onset of inflammation is immediate and the procedure is relatively straightforward. Even though they have limitations like all other models, they present some important immunological and histopathological aspects of IBD in humans [16]. The most widely used and characterized experimental model of erosion and inflammation related to UC in mice is the dextran sulphate sodium (DSS)-induced colitis, which is developed by DSS administration either in the drinking water [16, 17] or via intragastric catheter [18, 19]. The DSS induces a reproducible acute colitis [16]; however, there is some controversy regarding the type of inflammation that is induced. For some, the DSS model is recognized as a true model of colitis, while for others the model represents a model of epithelial erosion, but it is believed that DSS is directly toxic to gut epithelial cells of the basal crypts and affects the integrity of the mucosal barrier [11, 16, 20]. However, the model induces an acute colitis that is characterized by ulceration and infiltration, and also reflects many of the clinical features of IBD [11, 20–22]. For example, among other features, changing the DSS concentration or administration cycles can easily induce acute, chronic, and relapsing colitis. Our lab has extensive experience with this model [23–27].

The focus of most DSS studies has been on the dynamic and profile of mucosal response in relation to DSS treatment and its similarity to that observed in UC patients [11, 20–22]. These studies provide compelling evidence for changes in the gut mucosal immune response in mice treated with DSS compared to controls. In addition, other studies have investigated the role of defensins; antimicrobial, and anti-inflammatory components that are produced by paneth cells in the mucosa [28]. In this regard, mice with impaired expression of α-defensins due to destruction of the epithelium, and hence, the paneth cells, have been shown to be more susceptible to DSS-induced colitis, characterized by increased production of pro-inflammatory cytokines [28]. On the other hand, notable shifts in gut microbiota composition (dysbiosis) have been highlighted in IBD patients at different stages of the disease [29–32]. However, given the widespread use of DSS, not many studies have so far investigated the compositional shifts in gut microbiota and changes in their metabolic capacity in relation to DSS treatment in mice or rat models [33–42]. In this context, DSS treatment has been associated with changes in the composition of gut microbiota, whose dynamics shift toward an unhealthy state [33–37, 39, 41]. The nature of gut microbiota was also reported to influence sensitivity to acute DSS-induced colitis independently of host genotype [38]. In addition, interdependence of the mucosa-associated bacteria and chronic inflammation has also been reported [42]. Therefore, whether DSS-induced colitis causes dysbiosis or the nature of existing microbial colonization affects susceptibility to colitis remains a topic of discussion worth more explorations. It is however important to note that, most of the previous studies used 16S rRNA gene fingerprinting methods, such as terminal-restriction fragment-length polymorphism (T-RFLP), fluorescent *in situ* hybridization (FISH) [34–36, 38, 39, 42, 43], or sequencing of few clones per animal [35, 44], which had either low accuracy and precision or were limited in data mining. Furthermore, few studies investigated shifts in microbiota's functional potential or activity using metagenomic or metranscriptomic approaches [33, 37]. Therefore, a detailed and clear understanding of the structural and functional alterations of the intestinal microbiota in the DSS model is still required especially with the use of the high-throughput sequencing technologies.

The aim of the present study was to utilize Illumina sequencing of the 16S rRNA gene and inferred metagenomics by open source software PICRUSt (Phylogenetic Investigation of Communities by Reconstruction of Unobserved States [61]) to investigate differences in microbiome composition and function in the fecal and colonic mucosa of mice treated with 5% DSS for 5 days. We demonstrated that oral administration of DSS in C57Bl/6 mice significantly decreased bacterial species richness and shifted bacterial community composition. Specific taxa were associated with DSS treatment that may be important as intervention targets against the disease. In addition, DSS largely altered microbial activities and their functional pathways.

Materials and methods

Animals

Male C57BL/6 (7–9 weeks old) mice were purchased from Charles River (Senneville, QC, Canada) and maintained in

the animal care facility at the Faculty of Health Sciences, University of Manitoba. All experiments were approved by the University of Manitoba Animal Ethics Committee (10-073) and conducted according to the Canadian guidelines for animal research [45].

DSS colitis

DSS (molecular weight; MW 40 kDa: MP Biomedicals, Soho, OH, USA) was added to the drinking water at a final concentration of 5% (wt/vol) and administered for 5 days. Controls were time-matched and consisted of mice that received normal drinking water only. Five and four mice were included in the DSS and control groups, respectively.

Disease activity index

Disease activity index; DIA is the combined score for weight loss, stool consistency and bleeding, and the scores have historically correlated well with the pathological findings in DSS-induced model of IBD [46]. The scoring system was defined as follows: Weight: 0, no loss; 1, 5–10%; 2, 10–15%; 3, 15–20%; and 4, >20%; stool: 0, normal; 2, loose stool; and 4, diarrhea; and bleeding: 0, no blood; 2, presence of blood; and 4, gross blood. Blood was assessed using the Hemoccult II test (Beckman coulter, Oakville, ON, Canada). The DAI scoring was performed from days 0 to 5 over the period of DSS treatment.

Macroscopic scores

Mice were euthanized on day 6, at the end of d5 of DSS administration, the abdominal cavity was opened and the colon was located, isolated and opened longitudinally. Macroscopic damage was next evaluated on the full colon section, and macroscopic scores were assessed according to the rectal bleeding, rectal prolapse, diarrhea and colonic bleeding using a previously established scoring system [46].

Characterization of inflammation

Colon tissue samples were collected 5 days post-DSS activation, and blood was collected by intracardiac puncture under isoflurane (Abbot, Mississaugua, ON, Canada) anesthesia. Serum C-reactive protein (CRP); a marker for systemic inflammation was determined using an enzyme-linked immunosorbent assay (ELISA) commercial kit (R&D Systems, Minneapolis, MN, USA). Colonic samples were homogenized in 700 μl of Tris–HCl buffer containing protease inhibitors (Sigma, Mississauga, ON, Canada) and centrifuged for 12 min at 10,000 × g, and the supernatant was frozen at 80 °C until assay. Cytokine levels (IL-6, IL-1β) were determined using an ELISA commercial kit (R&D Systems).

DNA extraction and quality control

Approximately 200 mg of each fecal sample was used for DNA extraction using ZR fecal DNA extraction kit (Zymo Research Corp., Irvine, CA, USA). For colonic samples, the tissue was cut open and approximately 50 mg of mucosa scrapings were taken. DNA extraction from colonic mucosa samples was done using ZR Tissue and Insect DNA kit (Zymo Research Corp.). Both DNA extraction kits included a bead-beating step for the mechanical lysis of microbial cells. DNA was quantified using a NanoDrop 2000 spectrophotometer (Thermo Scientific, Wilmington, DE, USA). DNA samples were normalized to 20 ng/μl, and quality checked by PCR amplification of the 16S rRNA gene using universal primers 27F (5′-GAAGAGTTTGATCATGGCTCAG-3′) and 342R (5′-CTGCTGCCTCCCGTAG-3′) as described by Khafipour et al. [47]. Amplicons were verified by agarose gel electrophoresis.

Library construction and Illumina sequencing

The V4 region of 16S rRNA gene was targeted for PCR amplification using modified F515/R806 primers [48] as described previously [49]. In brief, a reverse PCR primer was indexed with 12-base Golay barcodes allowing for multiplexing of samples. The PCR reaction for each sample was performed in duplicate and contained 1.0 μl of pre-normalized DNA, 1.0 μl of each forward and reverse primers (10 μM), 12 μl HPLC grade water (Fisher Scientific, Ottawa, ON, Canada) and 10 μl 5 Prime Hot MasterMix (5 Prime, Inc., Gaithersburg, MD, USA). Reactions consisted of an initial denaturing step at 94 °C for 3 min followed by 35 amplification cycles at 94 °C for 45 s, 50 °C for 60 s, and 72 °C for 90 s; finalized by an extension step at 72 °C for 10 min in an Eppendorf Mastercycler pro (Eppendorf, Hamburg, Germany). PCR products were then purified using ZR-96 DNA Clean-up Kit (ZYMO Research) to remove primers, dNTPs and reaction components. The V4 library was then generated by pooling 200 ng of each sample, quantified by Picogreen dsDNA (Invitrogen, Burlington, NY, USA). This was followed by multiple dilution steps using pre-chilled hybridization buffer (HT1) (Illumina, San Diego, CA, USA) to bring the pooled amplicons to a final concentration of 5 pM, measured by Qubit 2.0 Fluorometer (Life technologies, Burlington, ON, Canada). Finally, 15% of PhiX control library was spiked into the amplicon pool to improve the unbalanced and biased base composition, a known characteristic of low diversity 16S rRNA libraries. Customized sequencing primers for

read1 (5′-TATGGTAATTGTGTGCCAGCMGCCGCGGTAA-3′), read2 (5′-AGTCAGTCAGCCGGACTACHVGGGTWTCTAAT-3′), and index read (5′-ATTAGAWACCCBDGTAGTCCGG-CTGACTGACT-3′) were synthesized and purified by polyacrylamide gel electrophoresis (Integrated DNA Technologies, Coralville, IA, USA) and added to the MiSeq Reagent Kit V2 (300-cycle) (Illumina). The 150 paired-end sequencing reaction was performed on a MiSeq platform (Illumina) at the Gut Microbiome and Large Animal Biosecurity Laboratories, Department of Animal Science, University of Manitoba, Winnipeg, MB, Canada. The sequencing data are uploaded into the Sequence Read Archive (SRA) of NCBI (http://www.ncbi.nlm.nih.gov/sra) and are accessible through accession number SRR2830596.

Bioinformatic analyses

The PANDAseq assembler [50] was used to merge overlapping paired-end Illumina fastq files. All the sequences with mismatches or ambiguous calls in the overlapping region were discarded. The output fastq file was then analyzed by downstream computational pipelines of the open source software package QIIME (Quantitative Insights Into Microbial Ecology) [51]. Chimeric reads were filtered using UCHIME [52] and sequences were assigned to Operational Taxonomic Units (OTU) using the QIIME implementation of UCLUST [53] at 97% pairwise identity threshold. Taxonomies were assigned to the representative sequence of each OTU using RDP classifier [54] and aligned with the Greengenes (v. 13.5) Core reference database [55] using PyNAST algorithms [56]. Phylogenetic tree was built with FastTree 2.1.3. [57] for further comparisons between microbial communities.

Alpha- and beta-diversity analyses

Within community diversity (α-diversity) was calculated by different indices of species richness and evenness such as Observed Number of Species, Chao1, ACE (abundance-based coverage estimators), Shannon, Simpson, InvSimpson, and Fisher using the open source R software. An even depth of 21,000 and 14,500 sequences per sample for fecal and colon mucosa samples, respectively, was used for the calculation of diversity indices. Beta-diversity was measured by calculating the weighted UniFrac distances using QIIME default scripts [58]. Principal coordinate analysis (PCoA) was applied on resulting distance matrices to generate two-dimensional plots using the open source R software (v. 3.1.0) and the p values were calculated using PERMANOVA analyses of Bray–Curtis distances [59]. Differences in alpha-diversity between DSS and control were determined using SAS (SAS 9.3, 2012). One colon sample in the control group was lost during DNA extraction and, therefore, only samples from three mice were included for all colon microbial analysis.

Partial least square discriminant analysis

Partial least square discriminant analysis (PLS-DA; SIMCA P+ 13.02, Umetrics, Umea, Sweden) was performed on genus data to identify the effects of DSS. As described previously [60], the PLS-DA is a particular case of partial least square regression analysis in which Y is a set of variables describing the categories of a categorical variable on X. In this case, X variables were bacterial taxa and Y was observations of different treatments compared together. To avoid over parameterization of the model, variable influence on projection value (VIP) was estimated for each genus, and genera with VIP <0.5 were removed from the final model. R^2 estimates then were used to evaluate the goodness of fit and Q^2 estimate was used to evaluate the predictive value of the model. Data were presented in loading scatter plots. The PLS-DA regression coefficients were used to identify taxa that were positively or negatively correlated with each treatment group.

Prediction of functional metagenome

The open source software PICRUSt (Phylogenetic Investigation of Communities by Reconstruction of Unobserved States; v. 1.0.0-dev) was used to predict the functional capacity of microbiome using 16S rRNA gene sequencing data and Greengenes (v. 13.5) reference database [61]. To make our open-reference picked OTUs compatible with PICRUSt, all de-novo OTUs were removed and only those that had matching Greengenes identifications were retained. The new OTU table was then used to generate metagenomic data after normalizing the data by copy numbers, and to derive relative Kyoto Encyclopedia of Genes and Genomes (KEGG) Pathway abundance [61]. The KEGG data were analyzed using STAMP (STatistical Analysis of Metagenomic Profiles) [62].

Statistical analysis

The UNIVARIATE procedure of SAS (SAS 9.3, 2012) was used to test the normality of residuals for α-diversity data. Data were used to assess the effect of treatment using MIXED procedure of SAS with treatment as the fixed and animal as the random factor (SAS 9.3, 2012). Phylum percentage data were also used to evaluate statistical differences between the DSS and control treatments. For the disease index activity, macroscopic scores, weight loss score and inflammatory markers, statistical analysis was performed using one-way ANOVA

followed by the Tukey–Kramer multiple comparison post hoc analysis, using prism (Prism 5, GraphPad, La jolla, CA, USA). The differences between groups were considered significant at $p < 0.05$.

Results

Macroscopic score, disease activity index, C-reactive protein, and cytokines IL-1β and IL-6

As shown in Fig. 1a–c, DSS increased disease activity index, weight loss score and macroscopic score ($p < 0.0001$). In this context, weight loss, and the presence of blood in the feces were increased whereas stool consistency was decreased. Also, the level of CRP, a marker of systemic inflammation, and inflammatory cytokines IL-1β and IL-6 increased in the DSS group ($p < 0.0001$; Fig. 1c–f). These results confirmed the presence of colitis in our DSS model.

Alpha-diversity of the fecal and colonic mucosa-associated microbiota (MAM)

Based on the different diversity indices used, DSS reduced bacterial species richness and evenness in the fecal samples compared to the control samples (Fig. 2a). Bacterial α-diversity in the colonic MAM was not significantly different between the control mice and the DSS mice samples, suggesting that both sample groups have similar bacterial species richness and evenness (Fig. 2b). The significance levels were determined using SAS and the p values are shown on top of each bar.

Beta-diversity in fecal and colon samples

As shown by the PCoA of weighted UniFrac distances, fecal samples clustered separately according to treatment group, suggesting that DSS and control samples were composed of distinct bacterial communities ($p = 0.007$; Fig. 3a). Although clustered separately for a large portion of communities, the colonic MAM still had an overlap of some bacterial communities, suggesting that DSS and control mice colon mucosa samples had shared bacterial communities ($p = 0.2$; Fig. 3b).

Microbiota composition at phylum and lower taxonomic levels in the fecal samples

A total of 259,126 sequences were generated after quality filtering steps with an average of 28,791 high-quality sequences per sample, which resulted in identification of 11 phyla and 86 taxa. Although most taxa were classified

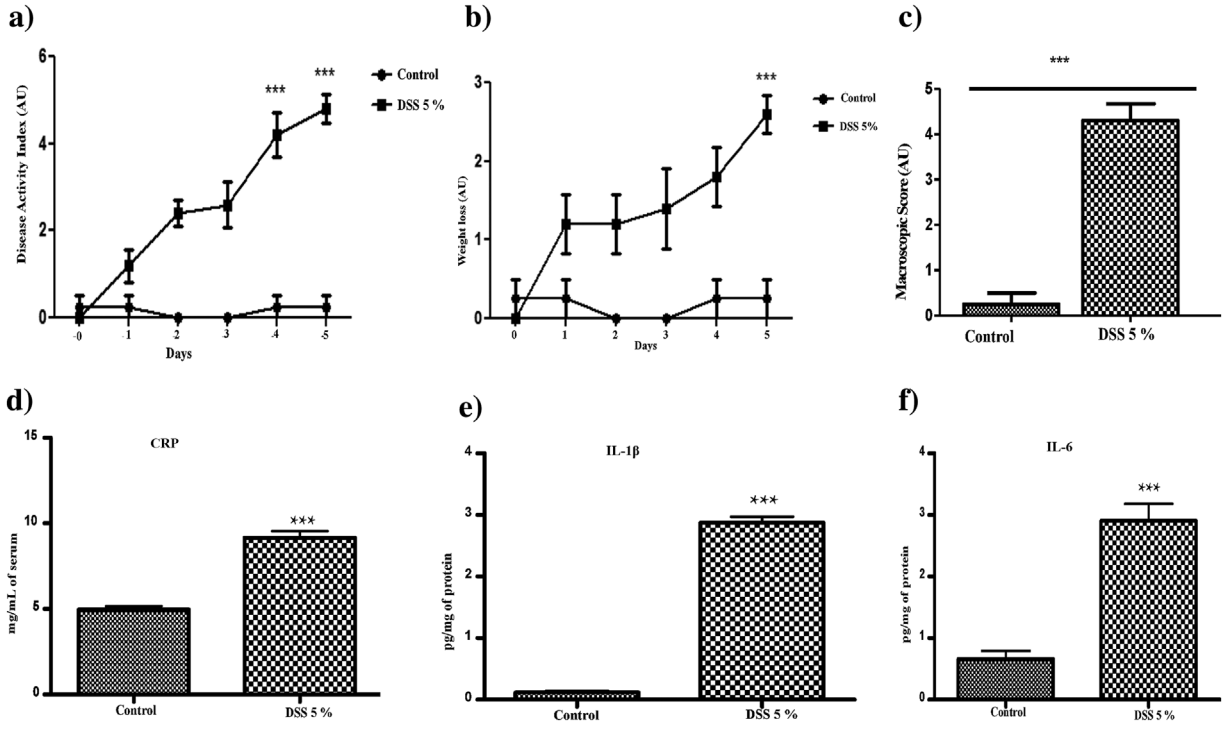

Figure 1. Dextran sulfate sodium (DSS)-induced colonic inflammation. Five percent DSS treatment for 5 days induced a significant increase in the; (a) disease activity index, (b) weight loss score, (c) macroscopic scores, (d) C-reactive protein (CRP), (e) IL-1β, and (f) IL-6. Values are shown as the mean ± SEM. AU, arbitrary units.

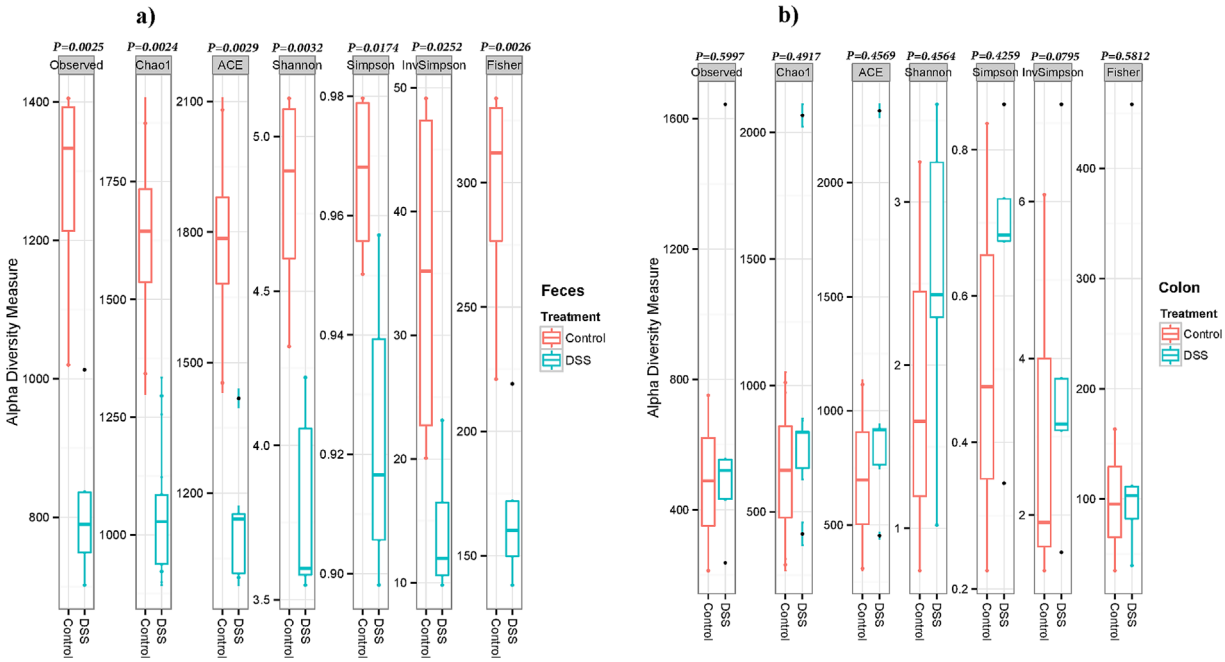

Figure 2. Alpha-diversity analysis, a measure of species richness and evenness based on different diversity indices, from dextran sulfate sodium-induced colitis and the control group studied at fecal and colon levels. (a) Fecal colitic samples had a lower bacterial diversity compared to non-colitic samples, suggesting that DSS reduced bacterial species richness. (b) Colonic mucosal bacterial diversity is not different between colitic and non-colitic samples, suggesting that both sample groups had similar bacterial species richness and evenness. The *p* values shown on top of each bar were calculated using SAS. DSS, dextran sulphate sodium.

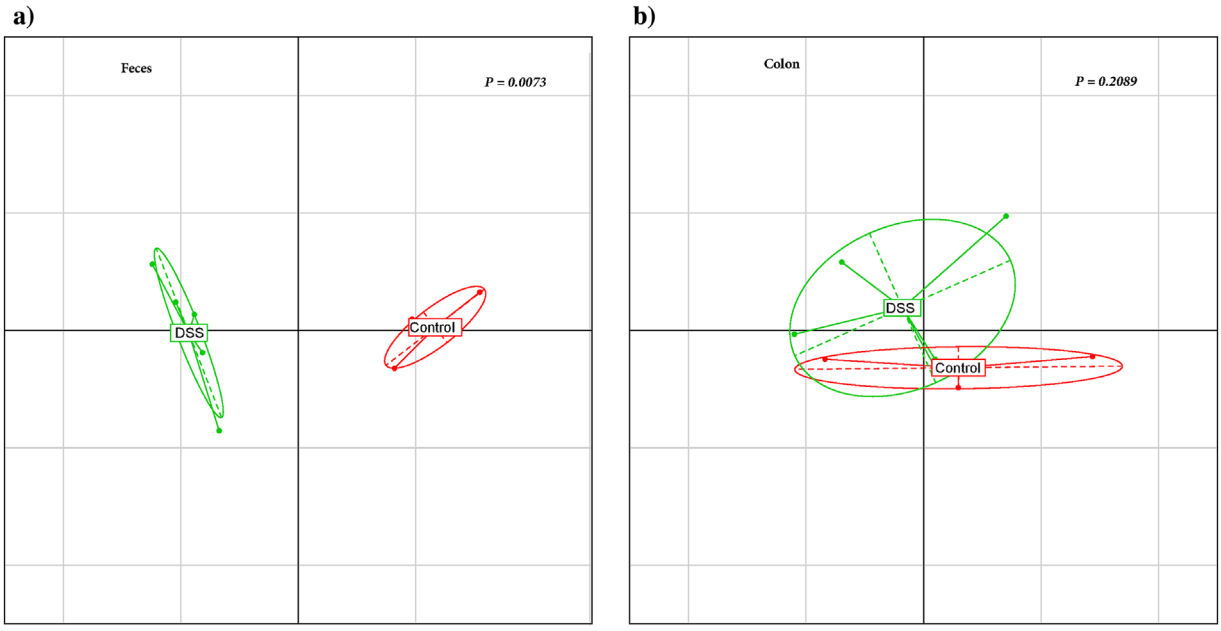

Figure 3. Principle coordinate analysis (PCoA) of weighted UniFrac distances, a measure of β-diversity of bacterial community. (a) Fecal samples clustered separately according to treatment status of the mice, suggesting that DSS and control mice samples are composed of distinct bacterial communities; (b) colon mucosa samples have shared bacterial communities. The *p* values were determined using PERMANOVA. DSS, dextran sulphate sodium.

at the genus (g.) level, some were only classified at the phylum (p.), class (c.), order (o.), or family (f.). Of the 11 phyla, six were abundant (≥1% of community), including Firmicutes, Bacteroidetes, Proteobacteria, Deferribacteres, Tenericutes, and Verrucomicrobia. The low-abundance phyla (<1% of community), included Actinobacteria, Cyanobacteria, Fibrobacteres, Spirochaetes, and TM7. Among the abundant phyla, DSS treatment reduced Bacteroidetes ($P = 0.01$) while Proteobacteria were increased ($p = 0.004$) compared to the control. Results of the relative abundances of various phyla are summarized in Fig. 4a.

Of the 86 taxa, 56 had abundance greater than or equal to 0.01% of community, whereas 30 were below 0.01%. Bacterial taxa with relative abundance of ≥0.01% of community were analysed using PLS-DA to identify bacteria that were most characteristic of the DSS or control treatments. As shown in Fig. 5a, *Bacteroides ovatus*, *Clostridium perfrigens*, *Helicobacter hepaticus*, and *Parabacteroides distasonis*; g. *Desulfovibrio*, *Escherichia*, *Helicobacter*, *Clostridium*, *Turicibacter*, *Parabacteroides*, *Bacilli*, *Allobaculum*, *Coprobacillus*, *Bacteroides*, *rc4-4*; and unclassified members of f. Enterobacteriaceae, Clostridiaceae, Bacteroidaceae; o. RF39, RF32, Bacteroidales, and Erysipelotrichales were positively correlated with the DSS group but negatively correlated with the control group. In addition, g. *Dessulfovibrio*, *Oscillospira*, *Odoribacter*, *Coprococcus*, *Dehalobacterium*, *Adlercreutzia*, *Lactobacillus*, *Prevotella*, *Bifidobacterium*; unclassified members of f. Lachnospiraceae, Lactobacillaceae, S24-7; and o. Lactobacillales were positively associated with the control group but negatively associated with the DSS group.

Microbiota composition at the phylum and lower taxonomic levels in colonic mucosa samples

A total of 199,057 sequences were generated after quality filtering steps with an average of 24,882 high-quality sequences per sample, which resulted in identification of 14 phyla and 151 taxa. Of the 14 phyla, five were abundant (≥1% of community), including Firmicutes, Bacteroidetes, Proteobacteria, Deferribacteres, and Verrucomicrobia. The low-abundance phyla (<1% of community), included Acidobacteria, Actinobacteria, Cyanobacteria, Fibrobacteres, Lentisphaerae, Planctomycetes, Spirochaetes, TM7, and Tenericutes. No significant difference was observed among the abundant phyla between DSS and control mice ($p > 0.05$). Results of the relative abundances of various phyla are summarized in Fig. 4b.

Of the 151 taxa, 68 had abundances greater than or equal to 0.01% of community, whereas 83 were below 0.01% of community. Bacterial taxa with relative abundance of ≥0.01% of community were analysed using PLS-DA to identify bacteria that were most characteristic of DSS or control treatments. As shown in Fig. 5b, *Lactobacillus reuteri*, *Bacteroides ovatus*; g. rc4-4, *Rikenellaceae*, *Bifidobacterium*, *YS2*, *Clostridium*; f. Bacteroidaceae, Clostridiaceae; o. RF32, RF39, Bacteroidales, Clostridales; and p. Proteobacteria were positively

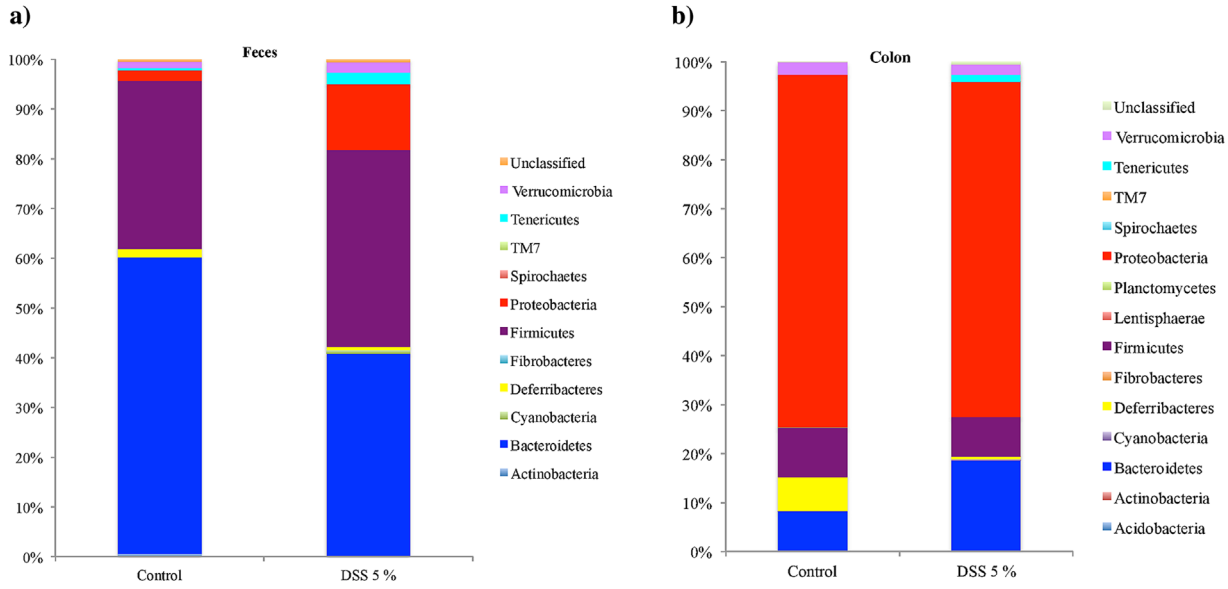

Figure 4. Percentage of relative abundances of bacterial phyla for: (a) fecal samples and (b) colon mucosa samples. The DSS significantly decreased Bacteroidetes and increased Proteobacteria in fecal samples but no significant difference was observed in the colonic mucosa samples. DSS, dextran sulphate sodium.

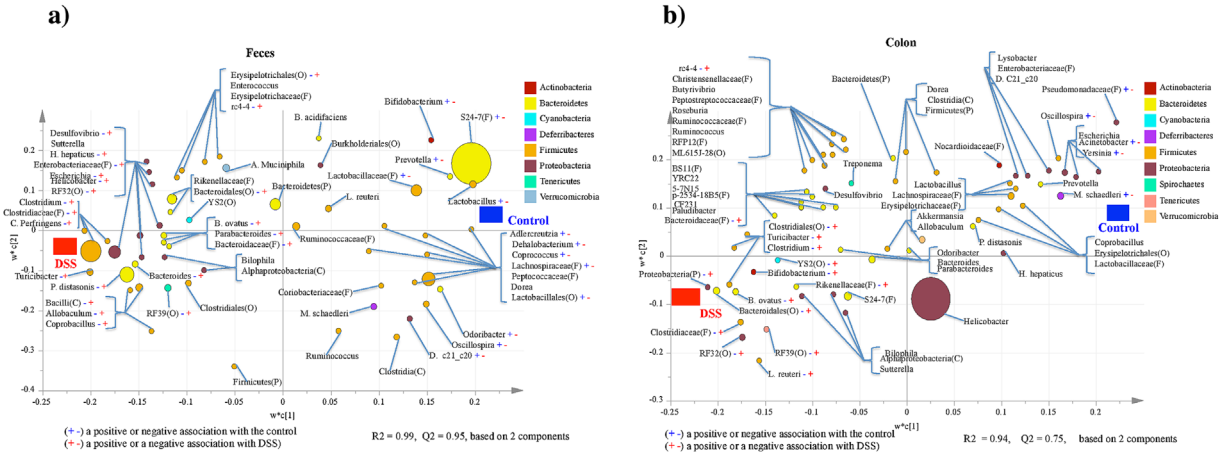

Figure 5. Partial least square discriminant analysis (PLS-DA) of bacterial communities comparing taxa that were associated with the control or DSS treatments in the mice's (a) fecal samples and (b) colon mucosal samples. All taxa are colored based on the phyla to which they belong to. The bubble size is representative of relative abundance of each taxa within the community. While majority of taxa were classified at the genus level, some could only be affiliated to phylum (P), class (C), order (O), or family (F) levels. – or + signs and their color are indicative of significant negative or positive association between each taxon and the associated group. DSS, dextran sulphate sodium.

associated with DSS, but negatively associated with the control. Also, *Mucispirillum schaedleri*; g. *Oscillospira, Acinetobacter*, *Yersinia*; and f. Pseudomonadaceae were positively associated with the control but negatively associated with the DSS.

Functional metagenome of colonic MAM and fecal microbiome

The analysis provided insights into functional shifts in the murine intestinal microbiome. A number of metabolic pathways were highly enriched in the colonic MAM and fecal microbiome in the DSS-treated mice compared to the control. In this context, the fecal microbiome of DSS-treated mice was associated with but not limited to, increased fatty acid biosynthesis, lysine degradation, pyruvate metabolism, propanoate metabolism, replication, recombination and repair proteins, and transcription machinery (Fig. 6a). In addition, the colonic MAM of the DSS-treated mice was associated with increased DNA repair and recombination proteins, peptidoglycan biosynthesis, DNA replication proteins, alanine, aspartate and glutamate metabolism, ribosome biogenesis, and several other pathways (Fig. 6b).

Discussion

The indigenous gut microbiota are thought to play a key role in the pathogenesis of IBD. Part of the evidence for the involvement of intestinal bacteria in IBD comes from studies with murine models of the disease supporting the hypothesis that a deregulated immune response against components of the intestinal microbiota is critically involved in the pathophysiology of IBD [11]. This is supported by the fact that antibiotic administration reduces the severity of disease in these models and rederivation of the mice to the germfree state prevents initiation of disease [63, 64]. Conversely, some germfree mice have been shown to have a high mortality rate when given DSS in drinking water as compared to conventional mice [63], suggesting that different subsets of normal microbiota may play certain roles in terms of the initiation, development or attenuation of disease.

We evaluated the fecal and colonic mucosal bacterial community dynamics, their functional alterations, as well as selected host variables in DSS-treated mice compared to control to elucidate which bacteria are most characteristic of DSS treatment, and which bacterial functional activities or metabolic pathways are affected. From the macroscopic assessment of disease severity in the colon, it was apparent that mice in the DSS-induced colitis treatment exhibited overt features of colitis compared to the healthy control group, which is in agreement with previous results where a DSS model was used [27, 36]. Also, analysis of the inflammatory markers including serum CRP level, a marker of systemic inflammation, showed significant differences between the two groups as DSS up-regulated this marker. In line with our findings, previous studies reported an extensive accumulation of neutrophils and an increase in the serum CRP level and colonic myeloperoxidase in DSS-colitis [27, 65]. We next considered other potential pro-inflammatory mediators that also play central role in

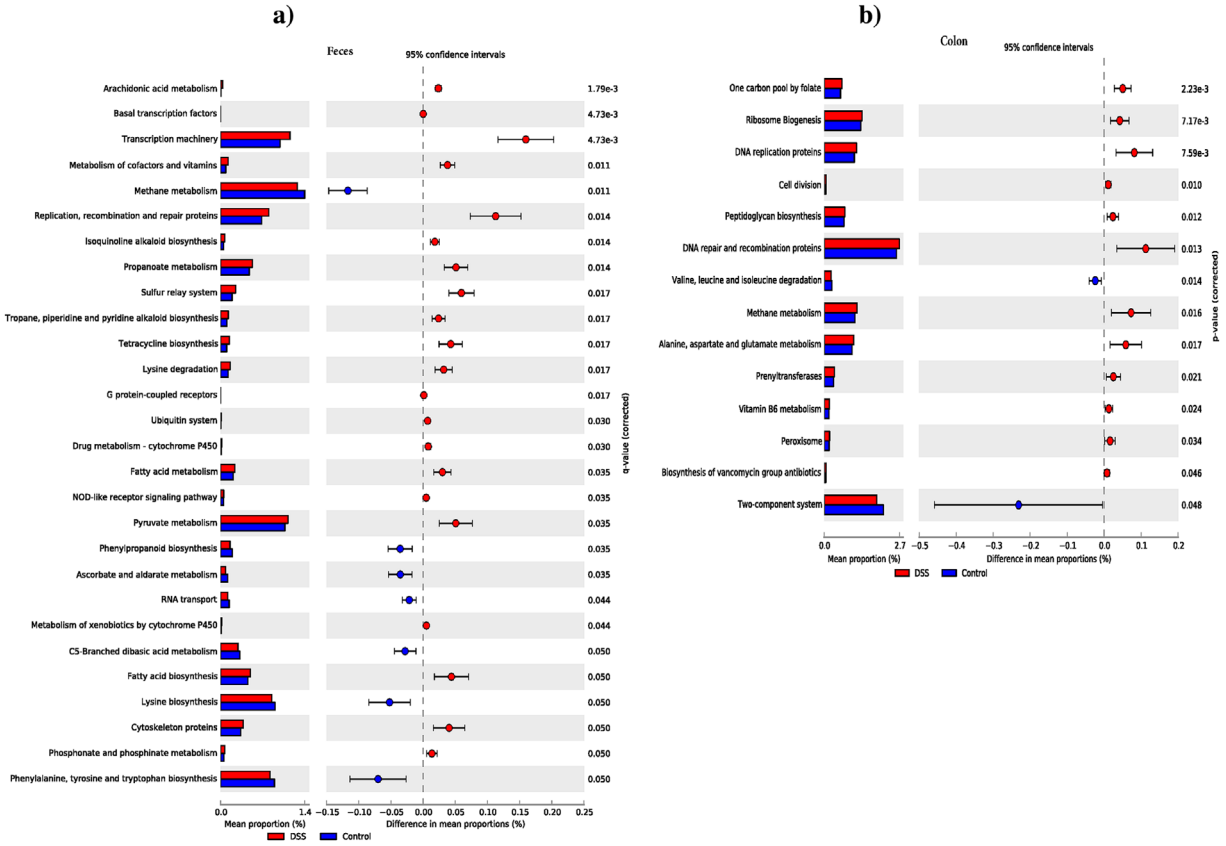

Figure 6. (a) Subsystems and pathways enriched or decreased within mice fecal samples isolated from colitic and non-colitic groups. Corrected *p* values were calculated using the Storey FDR correction. Subsystems or pathways overrepresented in the DSS or (control) fecal samples have a positive or (negative) difference between mean proportions and are indicated by red or (blue) coloring, respectively. (b) Subsystems and pathways enriched or decreased within mice colon samples isolated from the colitic and non-colitic groups. Subsystems or pathways overrepresented in the DSS or (control) mice colon samples have a positive or (negative) difference between mean proportions and are indicated by red or (blue) coloring, respectively.

the pathogenesis of IBD including UC and CD. The DSS significantly up-regulated inflammatory cytokines IL-1β and IL-6, a condition that has also been reported previously in colon of mice as a result of DSS-induced colitis [22, 27].

Decreased richness or diversity of bacterial species has been reported widely in both fecal and intestinal MAM samples of human patients with UC and CD, in intestinal MAM of dogs with IBD, and in fecal samples of rats with DSS-induced colitis [32, 36, 66–69]. This is consistent with our observation in fecal samples in which diversity analysis of bacterial species richness of the control and DSS-treated mice showed significant differences between these two groups. Also, our results on shifts in bacterial community composition are in agreement with Berry et al. [33], who reported differences in bacterial community composition in a pool of colonic and cecal contents of wild type mice, which was mostly a result of DSS treatment, although the authors did not find significant differences in α-diversity analysis. Furthermore, a loss of species diversity and a distinctive microbial community composition in intestinal MAM of DSS-treated mice [35] and in both fecal and intestinal MAM samples of humans with IBD [70] have also been reported. Interestingly, in our study, colonic MAM profiles from DSS-treated mice were not significantly different from bacterial profiles of the control mice in terms of bacterial richness and community composition at the phylum level. This may suggest possible differences in the effect of DSS on the richness and composition of microbiota at different anatomical sites or between mucosal and fecal samples. However, this was only limited to diversity and community composition at phylum level as bacterial differences were observed at lower taxonomical levels in both fecal and colon samples. This indicates that profiling of fecal and colonic bacteria by Illumina sequencing may be sensitive for investigating changes associated with

colitis and may reveal bacterial shifts at lower taxonomic levels that could otherwise be missed. In this regard, it was worth noting that more taxa were significantly associated with the DSS treatment in fecal samples compared to the colonic samples; however, several taxa including: *Bacteroides ovatus*, g. *Clostridium*, *rc4-4*; f. Clostridiaceae, Bacteroidaceae; and o. Bacteroidales, RF39, and RF32 were positively associated with the DSS treatment in both fecal and colonic mucosa samples. Some of these taxa have been reported to increase as a result of DSS [33], and although they may have different roles, their association with DSS in both colonic mucosa and in feces may indicate that they may play significant roles in the potentiation of the abnormal inflammatory response seen in DSS-treated animals, and could therefore be important as intervention targets against the disease. Lending support to these results, Berry et al. [33] also found that the overall abundances of the dominant phyla Firmicutes and Bacteroidetes were not affected by DSS treatment in mice, but taxa within the two phyla showed clear changes in abundance with respect to DSS treatment.

Members of the Bacteroidetes, such as o. Bacteroidales and f. Bacteroidaceae, have been identified as possible indicators of disease onset in the mouse model of colitis [37], and were also previously shown to be capable of inducing colitis in antibiotic-pretreated mice [71]. However, data on members of p. Bacteroidetes are more ambiguous, and thus, inconsistent findings have been reported for their presence in IBD compared to healthy controls [72–77]. Moreover, although still under investigations, some bacteria that were characteristic of DSS in the fecal samples, such as *Helicobacter hepaticus* and the f. Enterobacteriaceae, specifically g. *Escherichia*, have been implicated in IBD patients and in animal models of IBD [8, 31, 32, 37, 76, 78]. Similar findings for increased levels of Enterobacteriaceae have also been reported in murine colitis, and after antibiotic treatment or infection by enteric pathogens [44, 79, 80]. Therefore, a variety of conditions seem to drive the increase of Enterobacteriaceae, suggesting that the group may be a general indicator of a disrupted intestinal microbiota, but not necessarily a trigger of colitis [71]. However, there is strong data in support of the association of Enterobacteriaceae with IBD, especially CD. Generally, despite these differences in relative abundances of specific phylotypes, there appear to be a consensus in overall decrease in biodiversity in IBD patients and in murine models of colitis [33, 35, 68, 75].

The mechanisms by which DSS induced stronger bacterial shifts in the feces than in the colon mucosa are not fully understood. A similar observation has also been reported in IBD subjects whereby, changes in microbiome composition were more associated with the sample origin (stool or biopsy), and minor changes were observed in biopsy samples as opposed to stool samples [31]. It is possible that because DSS-induced colitis interferes directly with the intestinal epithelium and its barrier function as well as causing crypt damage [6, 22, 46, 81], this may lead to sloughing of mucosal epithelium, thereby decreasing the number of bacteria adhering to the mucosa, and consequently increasing the abundances of bacteria in the fecal matter.

Studies applying metagenomics, metatranscriptomics or metaproteomics investigating functional capacities of gut microbiota in humans [30, 31], and in mouse model of colitis [33], reported alterations in metabolic pathways that might affect host-microbiota interactions. These findings are in agreement with our results whereby, several alterations in microbial metabolic pathways in both the colon mucosa and fecal samples were observed. Given that the microbial analysis of diversity, community composition and also changes at phylum level for colonic samples did not show any significant difference between the DSS and control mice, the results suggest that analysis at microbial functional level might reveal important colitis-related changes in gut microbiome that are otherwise not noticeable at higher phylogenetic or community levels.

The microbial community shifts associated with IBD are still poorly understood, and intense investigation continues to determine whether these changes are responsible for disease etiology, or alternatively, an indirect consequence of IBD. However, we present a rigorous analysis of DSS-induced colitis, a commonly used animal model of UC that has analyzed microbial shifts and functional alterations in colonic mucosa and fecal samples. Although acute DSS colitis is different from UC, there are some similarities, such as shifts in microbiota composition, reduced species diversity and increment or decrease of specific groups of bacteria; therefore, the mechanistic outcome of this study might be relevant for research on human IBD. In this context, restoring microbial homeostasis by targeting colitis-associated taxa through specific microbiological interventions could form the basis for novel therapeutic strategies for IBD. Together, our data provide important insight into DSS-induced dysbiosis or perturbations in gut microbiota in the colonic and fecal samples, supporting the DSS model as a useful tool to examine the role of different bacteria in the pathogenesis of IBD.

Acknowledgments

This study was supported by grants from Crohn's and Colitis Canada, the Children's Hospital Research Institute of Manitoba, the Canada Foundation for Innovation, and the Canadian Institutes of Health Research to J.E.G., and a University of Manitoba start-up grant to E.K.

Conflict of interest

The authors have declared no conflict of interest.

References

[1] Cosnes, J., Gower-Rousseau, C., Seksik, P., Cortot, A., 2011. Epidemiology and natural history of inflammatory bowel diseases. Gastroenterology, **140**, 1785–1794.

[2] Manichanh, C., Borruel, N., Casellas, F., Guarner, F., 2012. The gut microbiota in IBD. Nat. Rev. Gastroenterol. Hepatol., **9**, 599–608.

[3] Strober, W., Fuss, I., Mannon, P., 2007. The fundamental basis of inflammatory bowel disease. J. Clin. Invest., **17**, 514–521.

[4] Basso, P.J., Fonseca, M.T.C., Bonfá, G., Alves, V.B.F., et al. 2014. Association among genetic predisposition, gut microbiota, and host immune response in the etiopathogenesis of inflammatory bowel disease. Braz. J. Med. Biol. Res., **47**, 727–737.

[5] Jager, S., Stange, E.F., Wehkamp, J., 2013. Inflammatory bowel disease: an impaired barrier disease. Langenbecks Arch. Surg., **398**, 1–12.

[6] Klag, T., Stange, F.E., Wehkamp, J., 2013. Defective antibacterial barrier in inflammatory bowel disease. Dig. Dis., **31**, 310–316.

[7] Hooper, L.V., Littman, D.R., Macpherson, A.J., 2012. Interactions between the microbiota and the immune system. Science, **336**, 1268–2273.

[8] Wallace, K.L., Zheng, L.B., Kanazawa, Y., Shih, D.Q., 2014. Immunopathology of inflammatory bowel disease. W. J. Gastroenterol., **20**, 6–21.

[9] Hibi, T., Ogata, H., Sakuraba, A., 2002. Animal models of inflammatory bowel disease. J. Gastroenterol., **37**, 409–417.

[10] Wirtz, S., Neurath, M.F., 2000. Animal models of intestinal inflammation- new insights into the molecular pathogenesis and immunotherapy of inflammatory bowel disease. Int. J. Colorectal. Dis., **15**, 144–1460.

[11] Wirtz, S., Neurath, M.F., 2007. Mouse models of inflammatory bowel disease. Adv. Drug Delivery Rev., **59**, 1073–1083.

[12] Elson, C.O., Cong, Y., Brandwein, S., Weaver, C.T., et al., 1998. Experimental models to study molecular mechanisms underlying intestinal inflammation. Ann. NY Acad. Sci., **859**, 85–95.

[13] Pizarro, T.T., Arseneau, K.O., Bamias, G., Cominelli, F., 2003. Mouse models for the study of Crohn's disease. Trends Mol. Med., **9**, 218–222.

[14] Elson, C.O., Sartor, R.B., Tennyson, G.S., Riddell, R.H., 1995. Experimental models of inflammatory bowel disease. Gastroentorology, **109**, 1344–1367.

[15] Sundberg, J.P., Elson, C.O., Bedigian, H., Birkenmeier, E.H., 1994. Spontaneous, heritable colitis in a new substrain of C3h/Hej mice. Gastroenterology, **107**, 1726–1735.

[16] Solomon, L., Mansor, S., Mallon, P., Donnelly, E., et al., 2010. The dextran sulphate sodium (DSS) model of colitis: an overview. Comp. Clin. Pathol., **19**, 235–239.

[17] Chassaing, B., Aitken, J.D., Malleshappa, M., Vijay-Kumar, M., 2014. Dextran sulfate sodium (DSS)-induced colitis in mice. Curr. Prot. Immunol., **104**, 15–25.

[18] Kim, C.J., Kovacs-Nolan, J.A., Yang, C., Archbold, T., et al., 2010. l-Tryptophan exhibits therapeutic function in a porcine model of dextran sodium sulfate (DSS)-induced colitis. J. Nutr. Biochem., **21**, 468–745.

[19] Lee, M., Kovacs-Nolan, J., Yang, C., Archbold, T., et al., 2009. Hen egg lysozyme attenuates inflammation and modulates local gene expression in a porcine model of dextran sodium sulfate (DSS)-induced colitis. J. Agric. Food Chem., **57**, 2233–2240.

[20] Kitajima, S., Takuma, S., Morimoto, M., 2000. Histological analysis of murine colitis induced by dextran sulfate sodium of different molecular weights. Exp. Anim., **49**, 9–15.

[21] Melgar, S., Karlsson, L., Rehnstrom, E., Karlsson, A., et al., 2008. Validation of murine dextran sulfate sodium-induced colitis using four therapeutic agents for human inflammatory bowel disease. Int. Immunopharmacol., **8**, 836–844.

[22] Yan, Y., Kolachala, V., Dalmasso, G., Nguyen, H., et al., 2009. Temporal and spatial analysis of clinical and molecular parameters in dextran sodium sulfate induced colitis. PLoS ONE, **4**, e6073.

[23] Ghia, J.E., Blennerhassett, P., Collins, S.M., 2007. Vagus nerve integrity and experimental colitis. Am. J. Physiol.: Gastrointest. Liver Physiol., **293**, G560–567.

[24] Ghia, J.E., Blennerhassett, P., El-Sharkawy, R.T., Collins, S.M., 2007. The protective effect of the vagus nerve in a murine model of chronic relapsing colitis. Am. J. Physiol.: Gastrointest. Liver Physiol., **293**, G711–718.

[25] Ghia, J.E., Blennerhassett, P., Kumar-Ondiveeran, H., Verdu, E.F., Collins, S.M., 2006. The vagus nerve: a tonic inhibitory influence associated with inflammatory bowel disease in a murine model. Gastroenterology, **131**, 1122–1130.

[26] Ghia, J.E., Li, N., Wang, H.Q., Collins, M., et al., 2009. Serotonin has a key role in pathogenesis of experimental colitis. Gastroenterology, **137**, 1649–1660.

[27] Rabbi, M.F., Labis, B., Metz-Boutigue, M.H., Bernstein, C.N., Ghia, J.E., 2014. Catestatin decreases macrophage function in two mouse models of experimental colitis. Biochem. Pharmacol., **89**, 386–398.

[28] Shi, J., 2007. Defensins and Paneth cells in inflammatory bowel disease. Inflamm. Bowel Dis., **13**, 1284–1292.

[29] Tamboli, C.P., Neut, C., Desreumaux, P., Colombel, J.F., 2004. Dysbiosis in inflammatory bowel disease. Gut, **53**, 1–4.

[30] Erickson, A.R., Cantarel, B.L., Lamendella, R., Darzi, Y., et al., 2012. Integrated metagenomics/metaproteomics reveals human host-microbiota signatures of Crohn's disease. PLoS ONE, **7**, e49138.

[31] Morgan, X.C., Tickle, T.L., Sokol, H., Gevers, D., et al., 2012. Dysfunction of the intestinal microbiome in inflammatory bowel disease and treatment. Genome Biol., **13**, (9):R79.

[32] Wills, E.S., Jonkers, D.M., Savelkoul, P.H., Masclee, A.A., et al., 2014. Fecal microbial composition of ulcerative colitis and Crohn's disease patients in remission and subsequent exacerbation. PLoS ONE, **9**, e90981.

[33] Berry, D., Schwab, C., Milinovich, G., Reichert, J., et al., 2012. Phylotype-level 16S rRNA analysis reveals new bacterial indicators of health state in acute murine colitis. ISME J., **6**, 2091–2106.

[34] De Fazio, L., Cavazza, E., Spisni, E., Strillacci, A., et al., 2014. Longitudinal analysis of inflammation and microbiota dynamics in a model of mild chronic dextran sulfate sodium-induced colitis in mice. W. J. Gastroenterol., **20**, 2051–2061.

[35] Nagalingam, N.A., Kao, J.Y., Young, V.B., 2011. Microbial ecology of the murine gut associated with the development of dextran sodium sulfate-induced colitis. Inflamm. Bowel Dis., **17**, 917–926.

[36] Samanta, A.K., Torok, V.A., Percy, N.J., Abimosleh, S.M., Howarth, G.S., 2012. Microbial fingerprinting detects unique bacterial communities in the faecal microbiota of rats with experimentally-induced colitis. J. Microbiol., **50**, 218–225.

[37] Schwab, C., Berry, D., Rauch, I., Rennisch, I., et al., 2014. Longitudinal study of murine microbiota activity and interactions with the host during acute inflammation and recovery. ISME J., **8**, 1101–1114.

[38] Brinkman, B.M., Becker, A., Ayiseh, R.B., Hildebrand, F., et al., 2013. Gut microbiota affects sensitivity to acute DSS-induced colitis independently of host genotype. Inflamm. Bowel Dis., **19**, 2560–2567.

[39] Hakansson, A., Tormo-Badia, N., Baridi, A., Xu, J., et al., 2015. Immunological alteration and changes of gut microbiota after dextran sulfate sodium (DSS) administration in mice. Clin. Exp. Med., **15**, 107–120.

[40] Liang, X., Li, H., Tian, G., Li, S., 2014. Dynamic microbe and molecule networks in a mouse model of colitis-associated colorectal cancer. Sci. Rep., **4**, 4985.

[41] Mar, J.S., Nagalingam, N.A., Song, Y., Onizawa, M., et al., 2014. Amelioration of DSS-induced murine colitis by VSL#3 supplementation is primarily associated with changesinileal microbiota composition. Gut Microbes, **5**, 494–503.

[42] Smith, P., Siddharth, J., Pearson, R., Holway, N., et al., 2012. Host genetics and environmental factors regulate ecological succession of the mouse colon tissue-associated microbiota. PLoS ONE, **7**, e30273.

[43] Heimesaat, M.M., Fischer, A., Siegmund, B., Kupz, A., et al., 2007. Shift towards pro-inflammatory intestinal bacteria aggravates acute murine colitis via Toll-like receptors 2 and 4. PLoS ONE, **2**, e662.

[44] Lupp, C., Robertson, M.L, Wickham, M.E., Sekirov, I., et al., 2007. Host-mediated inflammation disrupts the intestinal microbiota and promotes the overgrowth of Enterobacteriaceae. Cell Host Microbe, **2**, 119–129.

[45] Canadian Council on Animal Care, 1993. Guide to the Care and Use of Experimental Animals, 2nd ed. CCAC. Ottawa, Ontario, Canada. Vol. 1.

[46] Cooper, H.S., Murthy, S.N.S., Sedergran, D.J., Shah, R.S., 1993. Clinicopathologic study of dextran sulfate sodium experimental murine colitis. Lab. Invest., **69**, 238–250.

[47] Khafipour, E., Li, S., Plaizier, J.C., Krause, D.O., 2009. Rumen microbiome composition determined using two nutritional models of subacute ruminal acidosis. Appl. Environ. Microbiol., **75**, 7115–7124.

[48] Caporaso, J.G., Lauber, C.L., Walters, W.A., Berg-Lyons, D., et al., 2012. Ultra-high-throughput microbial community analysis on the Illumina HiSeq and MiSeq platforms. ISME J., **6**, 1621–1624.

[49] Derakhshani, H., Tun, H.M., Khafipour, E., 2016. An extended single-index multiplexed 16S rRNA sequencing for microbial community analysis on MiSeq illumina platforms. J. Basic Microbiol., **56**, 321–326.

[50] Masella, A.P., Bartram, A.K., Truszkowski, J.M., Brown, D.G., Neufeld, J.D., 2012. PANDAseq:PAaAired-eND assembler for illumina sequences. BMC Bioinf., **13**, 31.

[51] Caporaso, J.G., Kuczynski, J., Stombaugh, J., Bittinger, K., et al., 2010. QIIME allows analysis of high-throughput community sequencing data. Nat. Methods, **7**, 335–336.

[52] Edgar, R.C., Haas, B.J., Clemente, J.C., Quince, C., Knight, R., 2011. UCHIME improves sensitivity and speed of chimera detection. Bioinformatics, **27**, 2194–2200.

[53] Edgar, R.C., 2010. Search and clustering orders of magnitude faster than BLAST. Bioinformatics, **26**, 2460–2461.

[54] Wang, Q., Garrity, G.M., Tiedje, J.M., Cole, J.R., 2007. Naive Bayesian classifier for rapid assignment of rRNA sequences into the new bacterial taxonomy. Appl. Environ. Microbiol., **73**, 5261–5267.

[55] DeSantis, T.Z., Hugenholtz, P., Larsen, N., Rojas, M., et al., 2006. Greengenes, a chimera-checked 16S rRNA gene database and workbench compatible with ARB. Appl. Environ. Microbiol., **72**, 5069–5072.

[56] Caporaso, J.G., Bittinger, K., Bushman, F.D., DeSantis, T.Z., et al., 2010. PyNAST: a flexible tool for aligning sequences to a template alignment. Bioinformatics, **26**, 266–267.

[57] Price, M.N., Dehal, P.S., Arkin, A.P., 2010. FastTree 2 – approximately maximum-likelihood trees for large alignments. PLoS ONEne, **5**, e9490.

[58] Lozupone, C., Knight, R., 2005. UniFrac: a new phylogenetic method for comparing microbial communities. Appl. Environ. Microbiol., **71**, 8228–8235.

[59] Anderson M., 2005. PERMANOVA: a FORTRAN computer program for permutational multivariate analysis of variance. 24 ed. Department of Statistics, University of Auckland, New Zealand.

[60] Li, R., Khafipour, E., Krause, D.O., Entz, M.H., et al., 2012. Pyrosequencing reveals the influence of organic and conventional farming systems on bacterial communities. PloS One, **7**, e51897.

[61] Langille, M.G.I., Zaneveld, J., Caporaso, J.G., McDonald, D., et al., 2013. Predictive functional profiling of microbial communities using 16S rRNA marker gene sequences. Nat. Biotechnol., **31**, 814–821.

[62] Parks, D.H., Beiko, R.G., 2010. Identifying biologically relevant differences between metagenomic communities. Bioinformatics, **26**, 715–721.

[63] Rath, H.C., Schultz, M., Freitag, R., Dieleman, L.A., et al., 2001. Different subsets of enteric bacteria induce and perpetuate experimental colitis in rats and mice. Infect. Immun., **69**, 2277–2285.

[64] Sartor, R.B., 2008. Microbial influences in inflammatory bowel diseases. Gastroenterology, **134**, 5577–5594.

[65] Ghia, J.E., Blennerhassett, P., Collins, S.M., 2008. Impaired parasympathetic function increases susceptibility to inflammatory bowel disease in a mouse model of depression. J. Clin. Invest., **118**, 2209–2218.

[66] Andoh, A., Sakata, S., Koizumi, Y., Mitsuyama, K., et al., 2007. Terminal restriction fragment length polymorphism analysis of the diversity of fecal microbiota in patients with ulcerative colitis. Inflamm. Bowel Dis., **13**, 955–962.

[67] Frank, D.N., St Amand, A.L., Feldman, R.A., Boedeker, E.C., et al., 2007. Molecular-phylogenetic characterization of microbial community imbalances in human inflammatory bowel diseases. Proc. Natl. Acad. Sci. U. S. A., **104**, 13780–13785.

[68] Manichanh, C., Rigottier-Gois, L., Bonnaud, E., Gloux, K., et al., 2006. Reduced diversity of faecal microbiota in Crohn's disease revealed by a metagenomic approach. Gut, **55**, 205–211.

[69] Xenoulis, P.G., Palculict, B., Allenspach, K., Steiner, J.M., et al., 2008. Molecular-phylogenetic characterization of microbial communities imbalances in the small intestine of dogs with inflammatory bowel disease. FEMS Microbiol. Ecol., **66**, 579–589.

[70] Willing, B.P. Dicksved, J. Halfvarson, J. Andersson, A.F. et al., 2010. A pyrosequencing study in twins shows that gastrointestinal microbial profiles vary with inflammatory bowel disease phenotypes Gastroenterology, **139**, 1844–U105

[71] Bloom, S.M., Bijanki, V.N., Nava, G.M., Sun, L., et al., 2011. Commensal bacteroides species induce colitis in host-genotype-specific fashion in a mouse model of inflammatory bowel disease. Cell Host Microbe, **9**, 390–403.

[72] Andoh, A., Imaeda, H., Aomatsu, T., Inatomi, O., et al., 2011. Comparison of the fecal microbiota profiles between ulcerative colitis and Crohn's disease using terminal restriction fragment length polymorphism analysis. J. Gastroenterol., **46**, 479–486.

[73] Bibiloni, R., Mangold, M., Madsen, KL., Fedorak, R.N., Tannock, G.W., 2006. The bacteriology of biopsies differs between newly diagnosed, untreated, Crohn's disease and ulcerative colitis patients. J. Med. Microbiol., **55**, 1141–1149.

[74] Gophna, U., Sommerfeld, K., Gophna, S., Doolittle, W.F., Veldhuyzen van Zanten, S.J., 2006. Differences between tissue-associated intestinal microfloras of patients with Crohn's disease and ulcerative colitis. J. Clin. Microbiol., **44**, 4136–4141.

[75] Ott, S.J., 2004. Reduction in diversity of the colonic mucosa associated bacterial microflora in patients with active inflammatory bowel disease. Gut, **53**, 685–693.

[76] Sepehri, S., Kotlowski, R., Bernstein, C.N., Krause, D.O., 2007. Microbial diversity of inflamed and noninflamed gut biopsy tissues in inflammatory bowel disease. Inflamm. Bowel Dis., **13**, 675–683.

[77] Swidsinski, A., Ladhoff, A., Pernthaler, A., Swidsinski, S., et al., 2002. Mucosal flora in inflammatory bowel disease. Gastroenterology, **122**, 44–54.

[78] Munyaka, P.M., Sepehri, S., Ghia, J.E., Khafipour, E., 2016. Carrageenan gum and adherent invasive Escherichia coli in a piglet model of inflammatory bowel disease: impact on intestinal mucosa-associated microbiota. Front. Microbiol., **7**, 462.

[79] Hill, D.A., Hoffmann, C., Abt, M.C., Du, Y., et al., 2010. Metagenomic analyses reveal antibiotic-induced temporal and spatial changes in intestinal microbiota with associated alterations in immune cell homeostasis. Mucosal Immunol., **3**, 148–158.

[80] Stecher, B., Chaffron, S., Kappeli, R., Hapfelmeier, S., et al., 2010. Like will to like: abundances of closely related species can predict susceptibility to intestinal colonization by pathogenic and commensal bacteria. Plos Pathog., **6**, e1000711.

[81] Ni, J., Chen, S.-F., Hollander, D., 1996. Effects of dextran sulphate sodium on intestinal epithelial cells and intestinal lymphocytes. Gut, **39**, 234–241.